Please cite this article in press as: Sherman et al., Attention Robustly Gates a Closed-Loop Touch Reflex, Current Biology (2017), http://dx.doi.org/10.1016/j.cub.2017.05.058

Current Biology
Report

Attention Robustly Gates a Closed-Loop Touch Reflex

Dana Sherman,[1,2] Tess Oram,[1] David Harel,[2] and Ehud Ahissar[1,3,*]
[1]Department of Neurobiology, Weizmann Institute of Science, Rehovot 76100, Israel
[2]Department of Computer Science and Applied Mathematics, Weizmann Institute of Science, Rehovot 76100, Israel
[3]Lead Contact
*Correspondence: ehud.ahissar@weizmann.ac.il
http://dx.doi.org/10.1016/j.cub.2017.05.058

SUMMARY

Rats' large whiskers (macrovibrissae) are used to explore their nearby environment, typically using repetitive protraction-retraction "whisking" motions that are coordinated with head and body movements [1–8]. Once objects are detected, the rat can further explore the object tactually by using both the macrovibrissae and an array of shorter, stationary microvibrissae on the chin, as well as by using the lips [9–11]. When touch occurs during whisking, a fast reflexive response, termed a touch-induced pump (TIP), may be triggered. During a TIP, the whisker slightly retracts and protracts again, doubling the number of pressure onsets per contact. In head-fixed rats, TIPs occur in ~25% of the contacts [12]. Here we report that the occurrence of TIPs depends strongly on attention, indicated by head-turning toward an object: when rats intended to explore an object, either after encountering it during free exploration or when expecting its existence, the probability of a TIP increased from <30% to >65% without an increase in TIP latency. TIP regulation was unilateral and specific to the attended object; when two objects were palpated bilaterally simultaneously, TIP probability increased to >65% and decreased to <20% for contacts with the apparently-attended and apparently-unattended object, respectively. A data-driven computational model indicates that attentional gating could not be triggered by object contact, due to temporal constraints; rather, it could be based on a normally enabled or whisking-triggered scheme. Taken together, our results suggest that object-related attention regulates contact dynamics by gating the operation of a brainstem motor-sensory-motor loop and that this regulation is optimized for fast reaction.

RESULTS AND DISCUSSION

We analyzed the behavior of three rats that were freely exploring an arena containing one or two objects (Figure 1A; see STAR Methods). The objects were placed at random positions that were altered every two to three trials. Each trial (n = 82) was divided into several "encountering episodes" according to the number of times the rat initiated exploration of an object (total of 155 episodes). The first encountering episode of an object in a trial was termed the "first episode," and any later encountering episode of the already-explored object was termed a "late episode." In the following analysis, each episode consisted of a "pre-contact period," during which the rat explored the arena without touching any object, followed by a "contact period," during which the rat explored at least one object. Rats' behaviors were quantified by measuring head and whisker trajectories with respect to the objects (Figure 1B).

Head Turnings toward Objects

Object detection is often signaled by rapid head turning toward the object, turning that can be assumed to reflect a rapid shift of the rat's attention toward the detected object [2, 13, 14]. In our data, the average probability of observing head turning toward an object (HTO; STAR Methods) during first episodes before the first contact was P_{HTO} = 0.06. This probability increased abruptly to 0.54 immediately (<50 ms) after the first whisker-object contact (HTO1; STAR Methods) in first episodes (Figure 1C; $p < 10^{-5}$, t test; n = 61 episodes; see STAR Methods: Method Details, "HTO1 analysis").

Thus, in accordance with the literature, we consider HTO1 to be an orienting response [13] that indicates a shift in the rat's attention toward an object, and we base our analysis on this occurrence. Note that the converse—that attention necessarily involves HTO or HTO1—is not assumed here.

TIP Generation Dynamics

Whisking kinematics can be approximated as a modulated sinewave [15–20]. One of the major modulations of whisking kinematics is a rapid cycle of retraction-protraction appearing during the fundamental protraction period; these rapid cycles are termed "pumps" [4]. TIPs are a specific class of pumps that occur in response to contact, with delays (in head-fixed rats) of 18.1 ± 5.8 ms (mean ± SD) after contact [12]. In addition to the TIP response being limited to the ipsilateral side (see [12]), these short delays constrain the mechanism generating TIPs to be based in brainstem sensory-motor pathways [21], most likely in pathways activating retracting extrinsic muscles [22].

We examined the occurrence of TIPs during behavior as a function of fluctuations in attention, as determined by encounters with, and head turns toward, objects. All TIPs observed in this study occurred during protraction (313 out of 568 protractions with object contact), and none occurred during retraction (0 out of 52

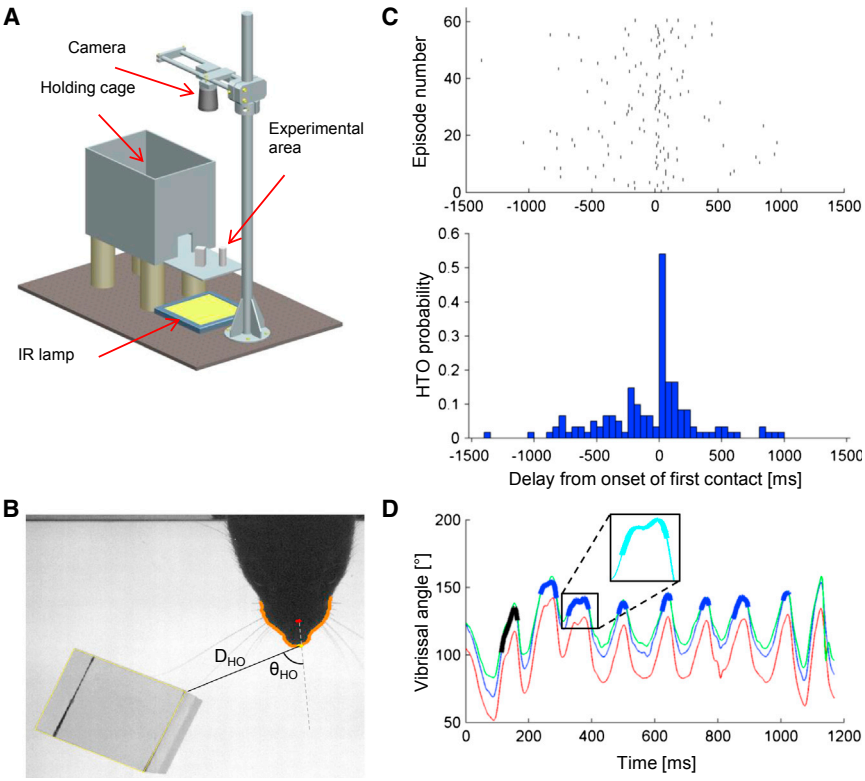

Figure 1. The Experimental Apparatus and Head and Whisker Motion Analyses

(A) The experimental apparatus (see STAR Methods).

(B) Quantification of head-object relationships. The angle between the midline axis of the head and the line connecting the tip of the snout (yellow dot) with a point marking the object (the closest vertex of a cube or the center of a cylinder) was defined as the angle between the head and the object (θ_{HO}); positive angles represent objects to the right of the snout. D_{Ho}, the distance (mm) between the tip of the snout and the point marking the object.

(C) Distribution of HTO latencies upon the first whisker-object contact during first episodes (n = 61 episodes). Raster plot (top; times of all HTOs in each episode are marked relative to first-contact onset time) and histogram (bottom; 50 ms bins) are shown.

(D) An exemplary trace of individual whiskers (left C1-3) before averaging. The full averaged trace is presented in Figure 2B. Inset: a higher-resolution example of an oTIP (averaged trace).

retractions with object contact) (Movies S1 and S2). TIPs were not necessarily triggered by contact with objects. In most late episodes and in some first episodes, TIPs were already generated during contacts with the floor before the first contact with the object (see STAR Methods). In the following sections, we analyze both object-triggered ("oTIPs") and floor-triggered ("fTIPs") TIPs. An example of whisker trajectories during an encountering episode is depicted in Figure 1D; an fTIP before object contact is followed by two oTIPs in each of the three fully tracked whiskers on the left side of the snout. In all consequent analyses, TIPs were computed as the mean trajectory of all fully tracked whiskers on the relevant side (e.g., inset in Figure 1D).

While exploring single objects in first episodes, rats generated more TIPs in contacts that followed the HTO1 than before it. On average, the probability of generating a TIP (P_{TIP}; defined as probability per cycle) was low before the first contact, remained low upon first contact, and increased only and immediately after HTO1 (P_{TIP} before/after the first contact refers to fTIPs/oTIPs; Figures 2A and 2C). The probability of generating the first TIP immediately following HTO1 was significantly larger than the probability of generating it during the first contact (P_{TIP} = 0.74 versus P_{TIP} = 0.29, respectively; p = 0.0004, n = 19 and n = 51 episodes, respectively; STAR Methods: Method Details; Table S3; Figure 2D). In contrast to first episodes, high levels of P_{TIP} were already observed during first contacts of late episodes (P_{TIP} = 0.71, n = 24 episodes; STAR Methods: Method Details; Table S3; Figures 2B and 2E). During late episodes, P_{TIP} was already relatively high during the pre-contact period and gradually increased toward the first contact (Figure 2F). While pre-contact and first-contact P_{TIP} levels differed between first and late episodes, TIP-generation latency was preserved (16.62 ± 3.77 versus 15.33 ± 3.36 ms in first (n = 16) versus late (n = 18) episodes; p = 0.3, t test; STAR Methods: Method Details; Table S3; Figure 2G).

To rule out the possibility that the TIP-HTO1 relation in first episodes is simply a vestibular effect independent of attention, we also analyzed TIP probability during the cycle that immediately followed HTOs that occurred during the pre-contact period ("pre-contact HTOs"; see STAR Methods: Method Details, "pre-contact HTO PTIP"; Table S3). In these cases, TIP generation was triggered by whisker-floor contacts. The PTIP following pre-contact HTOs was significantly lower than the PTIP following HTO1s (PTIP = 0.29 versus PTIP = 0.74, respectively; p = 0.0004, n = 34 and n = 19 first episodes, respectively), implying that the strong TIP-HTO1 relation is not simply a vestibular effect independent of attention.

Simultaneous Contacts with Two Objects

In 53 episodes, the rat was simultaneously touching two objects (e.g., Figures 3A and 3B and Movie S3). In episodes in which head turn toward one object occurred while simultaneously touching both objects, whisker motion on both sides was analyzed (n = 43 episodes; STAR Methods: Method Details). In these cases, the rat was either approaching the newly touched ("new") object while moving away from the already-inspected ("old") one (n = 32) or continuing to approach the old object, presumably ignoring the new one (n = 11). In the following, we refer to the approached object, new or old, as the "attended" object, and to the other as the "unattended" one.

P_{TIP} in whiskers on the side touching the attended object was significantly higher than that in whiskers on the side touching the unattended object (0.69 versus 0.20, p = 0.00002, n = 35 and n = 35; Table S3; Figure 3C). The transition of P_{TIP} between the two objects was sharp: P_{TIP} decreased sharply for the unattended object and increased sharply for the attended object

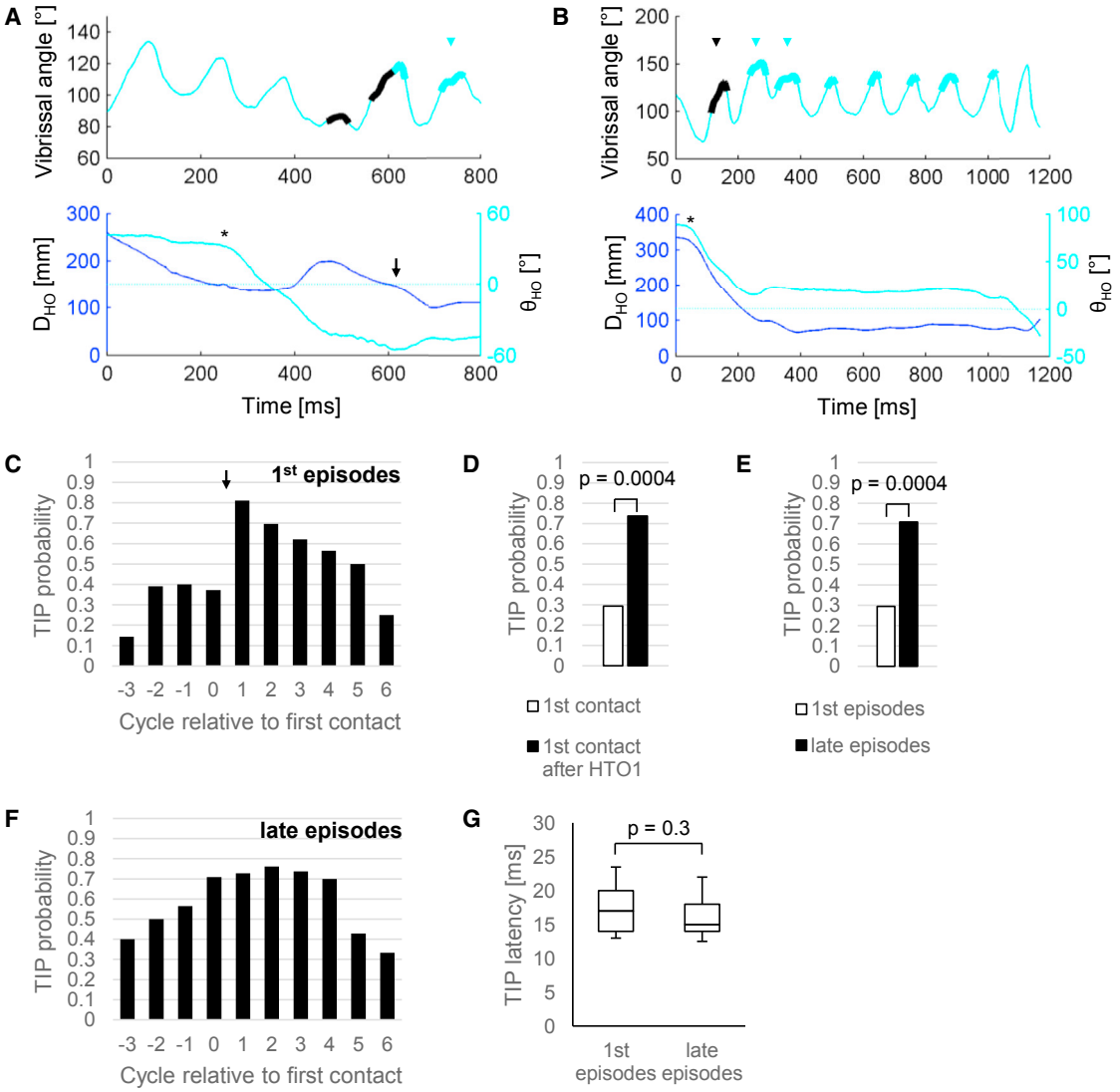

Figure 2. Palpation Behavior during First and Late Episodes

(A and B) Examples of a first (A; Movie S1) and a late (B; Movie S2) episode with object palpation. The average trajectory of all simultaneously tracked whiskers on the same side (right C1-2 in A and left C1-3 in B; see Figure 1D) is presented. Whisker-object contacts and whisker-floor contacts are indicated by bold cyan and bold black, respectively. All detected fTIPs and oTIPs are marked (black and cyan arrow tips, respectively). D_{HO} and θ_{HO} (see Figure 1B) are presented (A and B bottom, blue and cyan, respectively). All HTOs and HTO1 are marked by an asterisk and an arrow, respectively. Note that the HTOs occurred during the pre-contact period.

(C) P_{TIP} as a function of whisking cycle ordering relative to the contacting cycle during first episodes (n = 41; STAR Methods: Method Details). Negative whisking cycles represent cycles prior to the contact with the object and reflect fTIPs. Arrow marks the inter-contact interval in which HTO1 occurred.

(D) In first episodes, the probability of generating the first TIP during the first contact cycle and the cycle that immediately followed HTO1.

(E) P_{TIP} during the first contact cycle of first and late episodes.

(F) Same as (C), for late episodes (n = 26; STAR Methods: Method Details).

(G) Distributions of TIP-onset latency (from contact onset) during first contacts of first (n = 16) and late (n = 18) episodes (compared using t test).

See also Tables S1, S2, S3, and S6.

immediately after the HTO1 toward the attended object (Figure 3D). Importantly, the difference in P_{TIP} between the attended and unattended objects did not result from a difference in snout-object distance (Table S5).

Additional TIP Characteristics

P_{TIP} (in macrovibrissae) was high only when the macrovibrissae were the sole source of tactile information about the attended object. In many cases, palpation with the macrovibrissae continued also when the rat touched the object with its lips and cheek (e.g., Movie S4). In these cases (n = 23 episodes; STAR Methods: Method Details), P_{TIP} (0.13) did not significantly deviate from its baseline level (0.29 [n = 51 first episodes], p = 0.06, binomial test; Table S3).

While first-contact oTIPs were mostly generated in late episodes, these were also generated, at a lower probability, in first

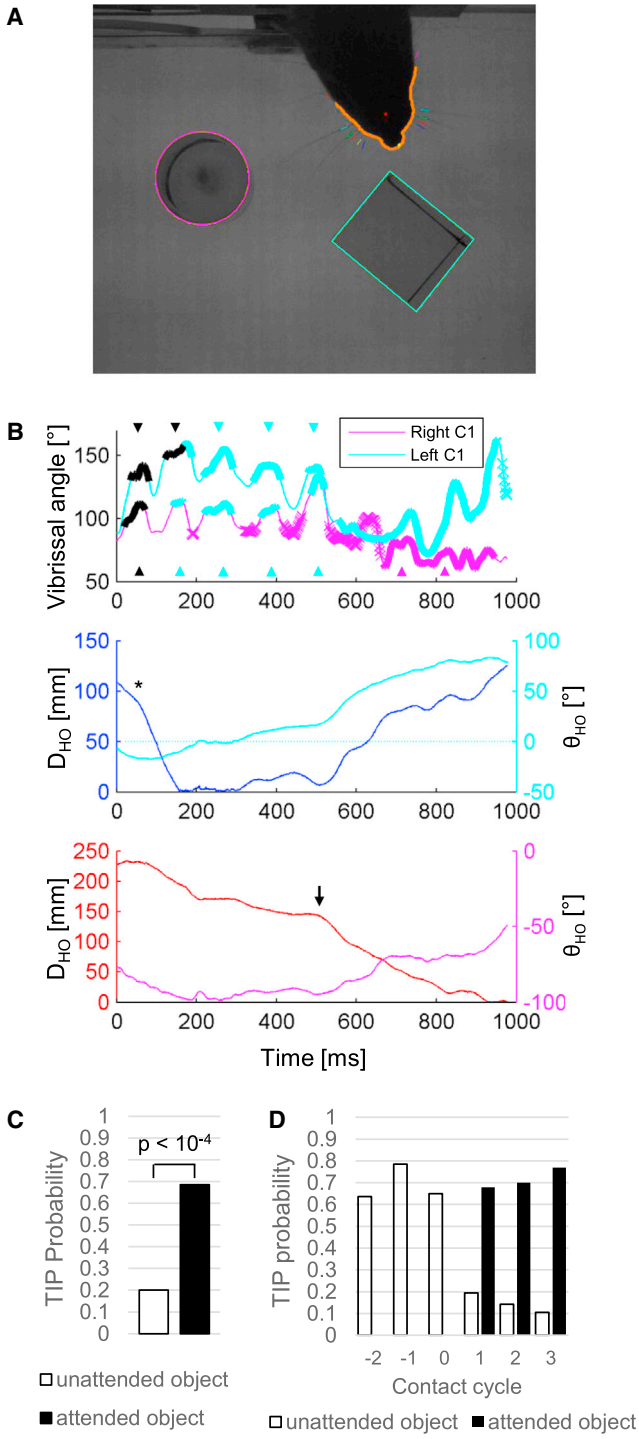

Figure 3. Palpation Behavior during Simultaneous Contacts with Two Objects

(A) The experimental setup. Two objects (cylinder and cube) were placed close enough to allow simultaneous contacts of contralateral whiskers with both.

(B) The trajectory of the most-caudal whisker on both the right (magenta) and left (cyan) sides of the snout are presented (top) (Movie S3). Contact of the whiskers with the cube and cylinder objects are indicated by bold cyan and bold magenta, respectively, and with the floor by bold black. Contact with an object with the back of the whiskers is indicated by "x." All detected fTIPs and oTIPs against the cube and cylinder are marked (black, cyan, and magenta arrow tips, respectively). D_{HO} and θ_{HO} (see Figure 1B) are presented for both objects (middle and bottom). HTOs and HTO1 are marked by an asterisk and an arrow, respectively.

(C) The probability of generating a TIP (P_{TIP}) on both sides of the snout during the first cycle of simultaneous contacts with two objects that immediately followed a head turn (HTO1) toward one of them (n = 35).

(D) Each bar shows the P_{TIP} for the unattended and attended objects during the i^{th} contact cycle, where i = 1 is the contact cycle that immediately followed the head turn toward the attended object (n = 43 episodes; STAR Methods: Method Details). There was not enough data to estimate the probabilities for the attended objects during the pre-HTO1 cycles.

See also Tables S1, S2, S3, and S5.

episodes (e.g., Figure 4A). The generation of first-contact oTIPs in first episodes was related to whisker motion during the preceding whisking cycle: first-contact oTIPs could be preceded by double-pump (DP; see STAR Methods), fTIP, or smooth protraction (see STAR Methods) in the cycle preceding contact. First-contact P_{TIP} was significantly higher following fTIPs than following smooth protractions (0.74 versus 0.33, $p < 0.05$, n = 19 and n = 15; Figure 4B). The reverse dependency was also significant: P_{TIP} of fTIPs was significantly higher than pre-contact smooth protractions when followed by first contacts with oTIPs (0.74 versus 0.26, $p = 0.002$, n = 19 and n = 19; STAR Methods: Method Details; Table S3). In addition, while the duration and amplitude of fTIPs were similar to those of first-contact oTIPs ($p > 0.19$), those of DPs were significantly larger ($p < 0.001$, t tests; Figure 4C). The tight coupling between pre-contact fTIPs and first-contact oTIPs, and their similar dynamics, supports switching to an attentive state that enables TIP occurrence upon any contact.

TIPs are often clustered across whisking cycles [12, 22]. The above observations are evident for all TIPs, regardless of their clustering context (Tables S1 and S2). Computational modeling predicts the occurrence of multiple TIPs within a single cycle in certain conditions [22]; our data confirm these predictions (Figure S1).

Possible Mechanisms for TIP Regulation

Our results demonstrate a significant increase in P_{TIP} following the first HTO1 in a trial (Figures 2C–2E). In addition, they display a lower P_{TIP} during pre-HTO1 cycles of first episodes than during pre-contact cycles of late episodes (Figure 2C versus Figure 2F). These results are consistent with TIPs being primarily associated with expected contacts. Importantly, however, not all expected contacts induced TIPs; these were primarily induced upon contacts with presumably attended objects (Figures 3C and 3D). The emerging hypothesis is thus that TIPs occur primarily when the vibrissal system intends to explore an object. Being in such a state enables TIP occurrence upon floor contacts as well (Figures 2B, 3B, and 4A, bold black).

We have used Statechart modeling [23] in order to test possible schemes for such attentive control, whose major constraint was to preserve the fast reaction time of TIPs (~16 ms; Figure 2G). We examined three schemes in which our brainstem model [22], a model that automatically generates TIPs at the correct latency following *every* whisker-object contact, can be modulated by attention in a manner that is consistent with our observations. Interestingly, the most straightforward scheme, in which

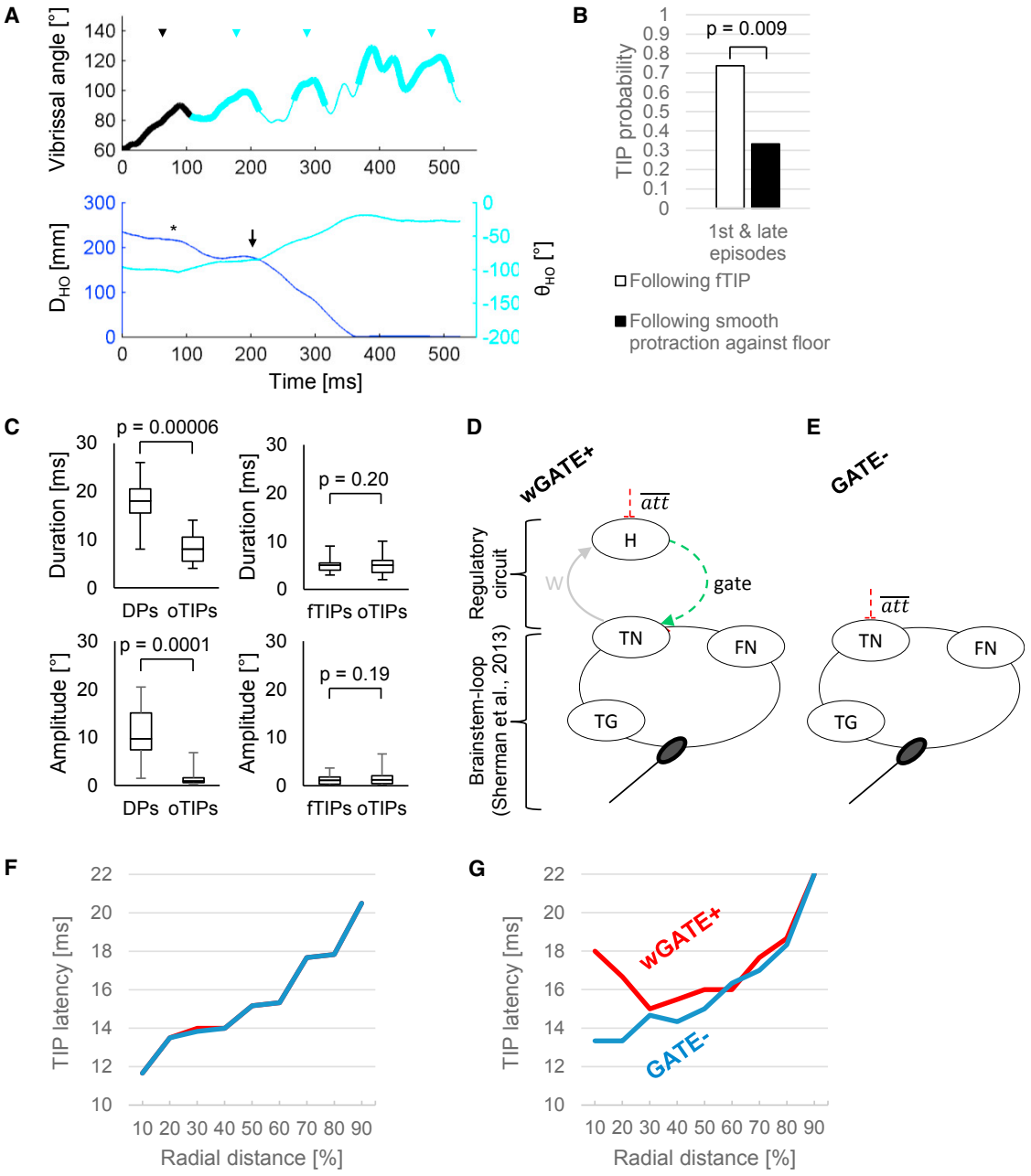

Figure 4. Pre-contact Kinematics and Possible TIP-Regulation Schemes

(A) Example of a first episode with an object that followed a pre-contact cycle with fTIP. The average trajectory of all tracked whiskers on the right side of the snout (C1-2) are presented (top). Whisker-object contacts and whisker-floor contacts are indicated by bold cyan and bold black, respectively. All detected fTIPs and oTIPs are marked (black and cyan arrow tips, respectively). D_{HO} and θ_{HO} (see Figure 1B) are presented (bottom). HTOs and HTO1 are marked by an asterisk and an arrow, respectively.

(B) TIP probability (P_{TIP}) during the first contact cycle of an episode, given fTIPs or smooth protraction during the preceding pre-contact cycle. The analyses include both first and late episodes (n = 34 episodes).

(C) Comparison of the kinematics (top, retraction duration; bottom, amplitude) of DPs (left, n = 12 episodes) and fTIPs (right, n = 17 episodes) versus oTIPs. DP or fTIP kinematics during the last pre-contact cycle were compared with the first oTIP (paired t tests).

(D and E) Plausible TIP-regulation schemes. A higher circuit regulates brainstem loop-mediated TIP generation [22] using whisking-dependent (D) or whisking-independent (E) attentional gating of the BS loop (see STAR Methods: Method Details). Lack of attention is indicated here by $\overline{att}$, a signal that is active in non-attentive conditions; other implementations are possible as well.

(D) Lack of attention ($\overline{att}$) disables a whisking-dependent (W) gating (gate) of TIP response.

(E) Lack of attention ($\overline{att}$) directly disables TIP response. In both schemes, whisker-object contacts can change the rat's attentiveness mode (not shown; see STAR Methods: Method Details). Dashed lines indicate pathways that are yet to be identified anatomically.

(legend continued on next page)

attentional switching occurs upon object contact, was ruled out based on temporal constraints (STAR Methods: Method Details). In contrast, two other schemes could preserve the observed short TIP delays while being consistent with the manner of attentional control observed here. In one of them, attentional switching occurs upon whisker-protraction onset (wGATE+, Figure 4D). In the other, the TIP "gate" is normally open and is inhibited by a lack of attention (GATE−, Figure 4E) (STAR Methods: Method Details). These results indicate that simple multiple-loop architectures can implement attentive control of low-level reflex loops without impairing their fast reaction time.

Although both proposed schemes are consistent with the existing data, their predicted behaviors differ for specific contact coordinate ranges (see simulation results in Figures 4F and 4G). Within the range of whisking amplitudes that can be simulated accurately [19], contacts that are proximal to the snout and that occur at small azimuthal angles (from the whisker's resting angle) are expected to induce TIPs at shorter latencies with the GATE− scheme (Figure 4G). Future examination of the dependency of TIP's latency on these specific combinations of azimuthal contact angles and radial distances can distinguish between these two schemes.

Overall, our results are consistent with TIPs being primarily associated with expected contacts and intentional object exploration. When expecting objects, TIPs are globally enabled prior to and during contact; after detecting one or more objects, TIPs are enabled only for contacts with the currently-attended object. Thus, consistent with previous conjectures [12, 22], our results suggest that TIP generation is state-ruled: the system switches between TIPs being enabled or not, a switching that is done separately for each side of the snout. This state-ruled process is shown to be implementable in the vibrissal system by a hierarchical loop network, in which the brainstem loop is gated by a higher loop in a way that does not increase its reaction time. Our data suggest that such top-down regulation serves the attentional preferences of the rat: attending a specific object "opens the TIPs' gate" for contacts against that object while closing the TIPs' gate for contacts with other objects. This is consistent with a view in which, at least in rodents, attention is integral to the sensorimotor circuits and is associated with preparing to move the sensor toward a selected object or location [13, 14, 24, 25]. In addition, the current results strongly suggest that TIPs are important components of object palpation, as they are enabled during attentive palpation. Why they are important, and what their functional uses are, remain to be studied.

Conclusions

We show that the fastest-known sensory-motor feedback process in the vibrissal system, the TIP reflex, functions under attentional control. When the rat intends to explore an object, either when encountering it during exploration or when expecting it, a fast TIP response is enabled. Our Statechart modeling captures the TIP behavior and its attentional control and suggests a plausible biological architecture in which its response dynamics are not impaired. The observed preference of the vibrissal system to allow TIPs when attentively exploring an object may be indicative of a perceptual function of TIPs.

STAR★METHODS

Detailed methods are provided in the online version of this paper and include the following:

- KEY RESOURCES TABLE
- CONTACT FOR REAGENT AND RESOURCE SHARING
- EXPERIMENTAL MODEL AND SUBJECT DETAILS
  - Experimental Apparatus
  - Behavioral Context
- METHOD DETAILS
  - Video Analysis and Encountering Episodes
  - Head Motion
  - Whisker Motion
  - Determination of First-Contact Onset Time
  - Inclusion Criteria for Video Analyses
  - The Model
  - Rationale of Model Expansion
  - Model Elements
  - Model Configurations
  - Simulated TIP Delays
  - Model Assumptions
  - Generality of the Multiple-Loop Model
  - Number of Elements in the Model
  - The Modeling Tools: Statecharts, Rhapsody, MATLAB
  - The Statechart of the Attentiveness Module
- QUANTIFICATION AND STATISTICAL ANALYSIS

SUPPLEMENTAL INFORMATION

Supplemental Information includes two figures and six tables and can be found with this article online at http://dx.doi.org/10.1016/j.cub.2017.05.058.

AUTHOR CONTRIBUTIONS

Conceptualization, D.S. and E.A.; Methodology, D.S., T.O., D.H., and E.A.; Formal Analysis, D.S.; Investigation, D.S. and T.O.; Writing – Original Draft, D.S. and E.A.; Writing – Review & Editing, D.S., T.O., D.H., and E.A.; Funding Acquisition, D.H. and E.A.

ACKNOWLEDGMENTS

We thank Dr. Enrico Segre, from the physics department of the Weizmann Institute, for providing the online acquisition software. This research was supported by the Israel Science Foundation (grants 1127/14 and 857/12), the Minerva Foundation funded by the Federal German Ministry for Education

(F and G) Latencies of the TIPs generated by the plausible TIP-regulation schemes. The average latency of TIP onset time during large (F, 7°–12°) and small (G, 4°–6°) azimuthal contact angles as a function of the radial distance of the object for the whisking-dependent (red) and whisking-independent (blue) attentional gating schemes. TIP latency is relative to contact-onset time. Azimuthal contact angle is relative to a whisker's angle at rest. Radial distance is relative to a whisker's length and is measured from the base of the whisker. A monotonous relation between the radial distance and the average TIP latency at large whisking amplitudes is shown for both schemes (F) and for the whisking-independent gating scheme alone at small amplitudes (G, blue). A deviation from monotonicity when both amplitude and radial distance of contact are small is shown for the whisking-dependent gating scheme (G, red).
See also Figures S1 and S2 and Table S4.

and Research, the Israel Ministry of Defense, the United States-Israel Binational Science Foundation (BSF, grant 2011432), and the NSF-BSF Brain Research EAGER program (grant 2014906). E.A. holds the Helen Diller Family Professorial Chair of Neurobiology. D.H. holds the William Sussman Professorial Chair in Mathematics.

Received: February 12, 2017
Revised: April 24, 2017
Accepted: May 17, 2017
Published: June 8, 2017

REFERENCES

1. Prescott, T.J., Diamond, M.E., and Wing, A.M. (2011). Active touch sensing. Philos. Trans. R. Soc. Lond. B Biol. Sci. *366*, 2989–2995.
2. Grant, R.A., Sperber, A.L., and Prescott, T.J. (2012). The role of orienting in vibrissal touch sensing. Front. Behav. Neurosci. *6*, 39.
3. Knutsen, P.M., Pietr, M., and Ahissar, E. (2006). Haptic object localization in the vibrissal system: behavior and performance. J. Neurosci. *26*, 8451–8464.
4. Towal, R.B., and Hartmann, M.J. (2006). Right-left asymmetries in the whisking behavior of rats anticipate head movements. J. Neurosci. *26*, 8838–8846.
5. Saraf-Sinik, I., Assa, E., and Ahissar, E. (2015). Motion makes sense: an adaptive motor-sensory strategy underlies the perception of object location in rats. J. Neurosci. *35*, 8777–8789.
6. Mitchinson, B., Martin, C.J., Grant, R.A., and Prescott, T.J. (2007). Feedback control in active sensing: rat exploratory whisking is modulated by environmental contact. Proc. Biol. Sci. *274*, 1035–1041.
7. Voigts, J., Herman, D.H., and Celikel, T. (2015). Tactile object localization by anticipatory whisker motion. J. Neurophysiol. *113*, 620–632.
8. Sofroniew, N.J., Cohen, J.D., Lee, A.K., and Svoboda, K. (2014). Natural whisker-guided behavior by head-fixed mice in tactile virtual reality. J. Neurosci. *34*, 9537–9550.
9. Brecht, M., Preilowski, B., and Merzenich, M.M. (1997). Functional architecture of the mystacial vibrissae. Behav. Brain Res. *84*, 81–97.
10. Hartmann, M.J., and Bower, J.M. (2001). Tactile responses in the granule cell layer of cerebellar folium crus IIa of freely behaving rats. J. Neurosci. *21*, 3549–3563.
11. Grant, R.A., Mitchinson, B., Fox, C.W., and Prescott, T.J. (2009). Active touch sensing in the rat: anticipatory and regulatory control of whisker movements during surface exploration. J. Neurophysiol. *101*, 862–874.
12. Deutsch, D., Pietr, M., Knutsen, P.M., Ahissar, E., and Schneidman, E. (2012). Fast feedback in active sensing: touch-induced changes to whisker-object interaction. PLoS ONE *7*, e44272.
13. Mitchinson, B. (2016). Tactile Attention in the Vibrissal System. In Scholarpedia of Touch (Springer), pp. 771–779.
14. Anjum, F., Turni, H., Mulder, P.G., van der Burg, J., and Brecht, M. (2006). Tactile guidance of prey capture in Etruscan shrews. Proc. Natl. Acad. Sci. USA *103*, 16544–16549.
15. Bermejo, R., Vyas, A., and Zeigler, H.P. (2002). Topography of rodent whisking–I. Two-dimensional monitoring of whisker movements. Somatosens. Mot. Res. *19*, 341–346.
16. Moore, J.D., Deschênes, M., Furuta, T., Huber, D., Smear, M.C., Demers, M., and Kleinfeld, D. (2013). Hierarchy of orofacial rhythms revealed through whisking and breathing. Nature *497*, 205–210.
17. Diamond, M.E., von Heimendahl, M., Knutsen, P.M., Kleinfeld, D., and Ahissar, E. (2008). 'Where' and 'what' in the whisker sensorimotor system. Nat. Rev. Neurosci. *9*, 601–612.
18. Wallach, A., Bagdasarian, K., and Ahissar, E. (2016). On-going computation of whisking phase by mechanoreceptors. Nat. Neurosci. *19*, 487–493.
19. Simony, E., Bagdasarian, K., Herfst, L., Brecht, M., Ahissar, E., and Golomb, D. (2010). Temporal and spatial characteristics of vibrissa responses to motor commands. J. Neurosci. *30*, 8935–8952.
20. Arkley, K., Grant, R.A., Mitchinson, B., and Prescott, T.J. (2014). Strategy change in vibrissal active sensing during rat locomotion. Curr. Biol. *24*, 1507–1512.
21. Matthews, D.W., Deschênes, M., Furuta, T., Moore, J.D., Wang, F., Karten, H.J., and Kleinfeld, D. (2015). Feedback in the brainstem: an excitatory disynaptic pathway for control of whisking. J. Comp. Neurol. *523*, 921–942.
22. Sherman, D., Oram, T., Deutsch, D., Gordon, G., Ahissar, E., and Harel, D. (2013). Tactile modulation of whisking via the brainstem loop: statechart modeling and experimental validation. PLoS ONE *8*, e79831.
23. Harel, D. (1987). Statecharts: a Visual Formalism for Complex-Systems. Sci. Comput. Program. *8*, 231–274.
24. Rizzolatti, G., and Craighero, L. (2010). Premotor theory of attention. Scholarpedia *5*, 6311.
25. Ahissar, E., and Assa, E. (2016). Perception as a closed-loop convergence process. eLife *5*, e12830.
26. Fonio, E., Gordon, G., Barak, N., Winetraub, Y., Oram, T.B., Haidarliu, S., Kimchi, T., and Ahissar, E. (2015). Coordination of sniffing and whisking depends on the mode of interaction with the environment. Isr. J. Ecol. Evol. *61*, 95–105.
27. Perkon, I., Kosir, A., Itskov, P.M., Tasic, J., and Diamond, M.E. (2011). Unsupervised quantification of whisking and head movement in freely moving rodents. J. Neurophysiol. *105*, 1950–1962.
28. Towal, R.B., and Hartmann, M.J. (2008). Variability in velocity profiles during free-air whisking behavior of unrestrained rats. J. Neurophysiol. *100*, 740–752.
29. Harel, D., and Gery, E. (1997). Executable Object Modeling with Statecharts. IEEE Computer *30*, 31–42.
30. Kleinfeld, D., Berg, R.W., and O'Connor, S.M. (1999). Anatomical loops and their electrical dynamics in relation to whisking by rat. Somatosens. Mot. Res. *16*, 69–88.
31. Kis, Z., Rákos, G., Farkas, T., Horváth, S., and Toldi, J. (2004). Facial nerve injury induces facilitation of responses in both trigeminal and facial nuclei of rat. Neurosci. Lett. *358*, 223–225.
32. Matyas, F., Sreenivasan, V., Marbach, F., Wacongne, C., Barsy, B., Mateo, C., Aronoff, R., and Petersen, C.C. (2010). Motor control by sensory cortex. Science *330*, 1240–1243.
33. Ahissar, E. (2008). And motion changes it all. Nat. Neurosci. *11*, 1369–1370.
34. O'Connor, D.H., Peron, S.P., Huber, D., and Svoboda, K. (2010). Neural activity in barrel cortex underlying vibrissa-based object localization in mice. Neuron *67*, 1048–1061.
35. Szwed, M., Bagdasarian, K., Blumenfeld, B., Barak, O., Derdikman, D., and Ahissar, E. (2006). Responses of trigeminal ganglion neurons to the radial distance of contact during active vibrissal touch. J. Neurophysiol. *95*, 791–802.
36. Szwed, M., Bagdasarian, K., and Ahissar, E. (2003). Encoding of vibrissal active touch. Neuron *40*, 621–630.
37. Saig, A., Gordon, G., Assa, E., Arieli, A., and Ahissar, E. (2012). Motor-sensory confluence in tactile perception. J. Neurosci. *32*, 14022–14032.
38. Bosman, L.W., Houweling, A.R., Owens, C.B., Tanke, N., Shevchouk, O.T., Rahmati, N., Teunissen, W.H., Ju, C., Gong, W., Koekkoek, S.K., and De Zeeuw, C.I. (2011). Anatomical pathways involved in generating and sensing rhythmic whisker movements. Front. Integr. Nuerosci. *5*, 53.
39. Aronoff, R., Matyas, F., Mateo, C., Ciron, C., Schneider, B., and Petersen, C.C. (2010). Long-range connectivity of mouse primary somatosensory barrel cortex. Eur. J. Neurosci. *31*, 2221–2233.
40. Hill, D.N., Curtis, J.C., Moore, J.D., and Kleinfeld, D. (2011). Primary motor cortex reports efferent control of vibrissa motion on multiple timescales. Neuron *72*, 344–356.
41. Yu, C., Derdikman, D., Haidarliu, S., and Ahissar, E. (2006). Parallel thalamic pathways for whisking and touch signals in the rat. PLoS Biol. *4*, e124.

42. Mink, J.W. (1996). The basal ganglia: focused selection and inhibition of competing motor programs. Prog. Neurobiol. *50*, 381–425.

43. Redgrave, P., Prescott, T.J., and Gurney, K. (1999). The basal ganglia: a vertebrate solution to the selection problem? Neuroscience *89*, 1009–1023.

44. Hires, S.A., Gutnisky, D.A., Yu, J., O'Connor, D.H., and Svoboda, K. (2015). Low-noise encoding of active touch by layer 4 in the somatosensory cortex. eLife *4*, e06619.

45. Towal, R.B., Quist, B.W., Gopal, V., Solomon, J.H., and Hartmann, M.J. (2011). The morphology of the rat vibrissal array: a model for quantifying spatiotemporal patterns of whisker-object contact. PLoS Comput. Biol. *7*, e1001120.

46. Haidarliu, S., and Ahissar, E. (1997). Spatial organization of facial vibrissae and cortical barrels in the guinea pig and golden hamster. J. Comp. Neurol. *385*, 515–527.

STAR★METHODS

KEY RESOURCES TABLE

REAGENT or RESOURCE	SOURCE	IDENTIFIER
Experimental Models: Organisms/Strains		
Albino Wistar rat	Envigo	HsdHan:WIST
Software and Algorithms		
IBM Rational Rhapsody	IBM	https://www.ibm.com/developerworks/downloads/r/rhapsodydeveloper/

CONTACT FOR REAGENT AND RESOURCE SHARING

Further information and requests for resources should be directed to and will be fulfilled by the Lead Contact, Ehud Ahissar (ehud.ahissar@weizmann.ac.il).

EXPERIMENTAL MODEL AND SUBJECT DETAILS

The whisking patterns of albino Wistar male rats (n = 3), aged 3-6 months, were measured. All whiskers were trimmed, except for one row (C-row) on each side of the snout. This configuration was chosen to simplify the tracking and analysis of whisker motion. On the day prior to behavioral recording, trimmed whiskers were clipped close to the skin (~1 mm) under Dormitor anesthesia (0.05 ml/100 g, S.C.).

Experimental Apparatus

Behavioral experiments were performed in a darkened, quiet room. The behavioral apparatus consisted of a holding cage (25 cm width, 35 cm length, 29.5 cm height), with a small door (6.9 cm height, 6 cm width), through which the rats could emerge into the experimental area (18 cm x 20 cm) [26](Figure 1A). Both the holding cage and the experimental area were fixed approximately 15 cm above the surface of a table. The experimental area consisted of a Perspex plate with 1–2 objects (Perspex cubes and cylinders) placed on it. The location of the objects was altered between trials. The Perspex plate was back-lit by an IR-lamp (880 nm wavelength, 23 cm x 23 cm, Metaphase). The experimental area was filmed from above by a high-speed, high-resolution camera (1280 × 1024 pix, 500 fps, CL60062, Optronics). An in-house program (E. Segre, Weizmann Institute) triggered the high-speed camera whenever the rat emerged from the holding cage into the experimental area. Video recording stopped when the rat returned to the holding cage.

Behavioral Context

An experimental session consisted of recording an untrained animal's whisking behavior whenever the rat was in the experimental area, over a period of 30–120 min. Preceding a session, the animal was placed in the holding cage for a 15 min acclimation period. During the acclimation period, the door of the holding cage was blocked. The experimental session began with unblocking the door to allow the animal to leave the holding cage and explore the experimental area at will. Each trial started with the rat moving from the holding cage to the experimental area, and ended with the rat going back into the holding cage. The length of the experimental session varied, depending on the animal's behavior and the amount of recorded video. The experimenter's interference and contact with the animal were minimized during the experimental session, and there was no interference or contact while the animal was in the experimental area. All experimental protocols were approved by the Institutional Animal Care and Use Committee of the Weizmann Institute of Science.

METHOD DETAILS

Video Analysis and Encountering Episodes

All raw video records were analyzed visually by two independent observers; periods with sufficient visual quality were also quantitatively analyzed using the BIOTACT Whisker Tracking Tool after low-pass filtering at 60 Hz [http://bwtt.sourceforge.net; [27]). All untrimmed whiskers were individually tracked. The trajectories of all unilateral whiskers that were fully tracked throughout each inspected time period were averaged for quantitative analysis. Each trial (n = 82 in total for all 3 rats together) was divided into several "encountering episodes", each including a "contact period", defined as a period during which the rat focused its whisking on an object and continuously whisked on that object with no whisking cycle without contact, preceded by a "pre-contact period", during which the rat explored the arena without touching any object. The first encountering episode with an object on a trial was termed the

"first episode" and any later encountering episode of the already-explored object was termed a "late episode". For both first- and late episodes, the switching from pre-contact- to contact period was upon protraction-onset of the first contact cycle between at least one whisker and the inspected object(s). First-contact time was defined as contact-onset time of the whisker(s) that touched the object(s) first (and see "Determination of first-contact onset time"). In episodes in which only one object was inspected, the trajectories of only the whiskers on the side that touched the object first were analyzed, and in episodes in which two objects were inspected simultaneously the trajectories of the whiskers on both sides of the snout were analyzed. The contact period ended when the rat moved away from at least one of the inspected objects and the whiskers on the analyzed side no longer touched the object(s).

Head Motion

Head motion was tracked continuously and was quantified by two variables: head-object distance, D_{HO}, and the change in head-object angle (θ_{HO}), i.e., rotational velocity, ω_{HO} (Figure 1B). Two lines were used to quantify both variables: (1) the line connecting the tip of the snout and the inspected object (Figure 1B, solid black line), and (2) the line connecting the tip- and the center of the snout (Figure 1B, dashed gray line). The length of the first of these was defined as the head-object distance, D_{HO}, and the temporal derivative of the absolute angle between the two lines defined the rotational velocity of the head relative to the object, ω_{HO}. Points along the trajectory of head motion were classified as "head turning toward an object" (HTO) when D_{HO} decreased and ω_{HO} was one standard deviation above the mean of ω_{HO} (56°/sec; ω_{HO} was normally distributed). The first HTO that occurred following the first whisker-object contact during an episode was classified as "HTO1".

Whisker Motion

Whisker protraction was classified as either "smooth protraction", "double-pump" (DP), or "touch-induced pump" (TIP), depending on the existence of contact and on the angular acceleration during whisker protraction. Whisker protraction was classified as DP (or TIP) if there was a period of negative angular acceleration during free-air (or during whisker-object contact) protraction that was preceded and followed by positive angular acceleration [28]. Whisker-floor contacts were identified when: (a) the tip of at least one whisker bent significantly, (b) the whisker(s) stopped protracting, and (c) the distance between the tip of the snout and the center of the snout (Figure 1B, red dot) decreased. Whisker motion that was not classified as either a DP or a TIP was classified as smooth protraction. Similar definitions, with reversed movement directions, were used for retraction periods.

Determination of First-Contact Onset Time

The criteria for defining the time of first contact were: the first frame during whisker protraction in which at least one of the whiskers on the touching side fulfilled all of the following: (1) changed its curvature, and (2) slowed down. Range of error estimation of first-contact time was 1-7 ms, with median and IQR of 4 and 2 ms, respectively (Table S6).

Inclusion Criteria for Video Analyses

Pre-contact HTO P_{TIP} Analysis

(1) The episode included a pre-contact period; (2) this pre-contact period included an HTO ("pre-contact HTO"); (3) the whisking cycle that immediately followed the pre-contact HTO included a whisker-floor contact; (4) the episode was the first episode in a trial (for better comparison with the TIP-HTO1 relation); (5) whisker motion during the analyzed contact cycle was unambiguous. Accordingly, out of 58 potential pre-contact HTOs, 34 were included in the analysis.

HTO1 Analysis

(1) The episode included a pre-contact period; (2) the rat was touching only one object during the contact period; (3) the first whisker-object contact cycle was unambiguous. Accordingly, out of 115 and 40 potential first- and late episodes, 61 and 40, respectively, were included in this analysis.

First-Contact P_{TIP} Analysis

(1-3) as in HTO1 analysis; (4) the first whisker-object contact occurred during protraction; (5) whisker motion during the first contact cycle was unambiguous. Accordingly, out of the 61 and 40 potential first- and late episodes that were included in the HTO1 analysis, 51 and 24, respectively, were included in this analysis.

First-Contact TIP Latency Analysis

(1-5) as in first-contact P_{TIP} analysis; (6) first- and late episodes included a first-contact TIP. Accordingly, out of the 51 and 24 potential first- and late episodes that were included in the first-contact P_{TIP} analysis, 16 and 18, respectively, were included in this analysis.

HTO1 P_{TIP} Analysis

(1-4) as in first-contact P_{TIP} analysis; (5) the contact period included an HTO1. Note that these were always generated following the first contact, by definition; (6) the contact period included a whisker-object contact following the HTO1; (7) the episode was the first episode in a trial; (8) whisker motion during all analyzed contact cycles was unambiguous. Accordingly, out of the 51 potential first-episodes that were included in the first-contact P_{TIP} analysis, 19 were included in the analysis.

Single-Object P_{TIP}-Profile Analysis

(1-4) as in first-contact P_{TIP} analysis; (5) first episodes included an HTO1 (last episodes could either include an HTO1 or not); (6) the contact period did not include cycles with no whiskers-object contact. Accordingly, out of 61 and 40 potential first- and late episodes that were included in the first-contact P_{TIP} analysis, 41 and 26, respectively, were included in the analysis.

Two-Object P_{TIP} Analysis

(1) The simultaneous contact period included a head-turn toward one of the objects; (2) the simultaneous contact period was preceded by a contact period with only one of the objects, indicating the already-inspected object (see Results); (3) whisker motion was unambiguous. Accordingly, out of 53 potential cases, 43 were included in the analysis. These included 35 and 35 contacts with the newly- and already-inspected objects, respectively.

Two-Object P_{TIP}-Profile Analysis

(1-3) as in "Two-object P_{TIP}" analysis. Accordingly, as in "Two-object P_{TIP}" analysis, 43 were included in the analysis.

Face P_{TIP} Analysis

(1) The rat touched only one object during the contact period; (2) the rat switched from touching the object solely with its whiskers to touching it with its face (lips or cheek); (3) the rat approached the object when switching from vibrissal-aided to face-aided palpation; (4) the whiskers touched the object on the first face-object contact cycle; (5) whisker motion during face-object contacts was unambiguous. Accordingly, out of 41 potential cases, 23 were included in the analysis.

Floor P_{TIP} Analysis

(1) The whiskers on the analyzed side touched the floor during the last pre-contact cycle; (2) the first contact with the object occurred during protraction; (3) whisker motion was unambiguous. Accordingly, out of 155 (115 first- and 40 late-) potential episodes, 38 were included in the analysis.

Calculation of TIP-Cluster P_{TIP}

In order to avoid edge effects the first- and last TIP along the contact period were excluded from the TIP-cluster P_{TIP} calculation. P_{TIP} inside TIP clusters was calculated by dividing the total number of middle (non-edge) TIPs of all episodes that displayed TIP-clusters (n = 82 episodes), by the total number of middle contacts inside the clusters. Including also the edge TIPs gave the upper bound of TIP-cluster P_{TIP}.

The Model

This study was performed using an expanded version of our previously reported brainstem-loop (BS-loop) model [22], a computational model implemented in the visual language of statecharts [23], using the Rhapsody tool [29]. Two components were added in the expanded version, a higher loop (termed the H-loop) and an attentiveness module (termed X), applying top-down control on the BS loop.

Rationale of Model Expansion

Following our experimental results, we postulated that touch triggers two processes, TIP generation and TIP regulation. In order to regulate the automatic generation of TIPs by our simulated BS loop [22], we added to the model a higher loop (H-loop). This regulatory loop allowed a fast generation of TIPs in response to whisker-object contact, while assuring that these would occur only when the rat was touch-attentive, in order to be consistent with our empirical data. The attention-based regulation by the H-loop resulted from a top-down regulation of the H-loop, by the second element that was added to the model: an attentiveness module (X). In contrast to the H-loop, X responded slowly to whisker-derived inputs, assuring that TIPs would not occur right from the first contact if the rat was inattentive, in accordance with empirical data. Once it responded to the contact inputs, X changed its attentiveness mode for a long time, allowing fast generation of TIPs from the second contact on. X switched to its inattentive mode after several contact cycles, consistent with our empirical data (see TIP-cluster statistics). We should note that this two-level division is not absolutely mandatory, and the two new elements could have been combined (see Generality of the multiple-loop model). However, it is important to note that in our simulations a continuous excitatory input may cause spurious activations of the post-synaptic cells at uncontrolled times. Thus, avoiding the dual time-scale design and connecting the output of X directly to the BS loop would result in spurious activations of BS neurons at undesired times.

Model Elements

BS Loop

The BS-loop elements are described in detail in [22]. Briefly, the brainstem (BS) loop is a tri-synaptic loop [30, 31], in which signals from the vibrissae ascend the trigeminal nerve to primary sensory neurons in the trigeminal ganglion [Figures S2A–S2F, "TG"; termed SN1s in 22], the vibrissae-derived signals are transmitted to second-order sensory neurons in the trigeminal nuclei [Figures S2A–S2F, "TN"; termed SN2s in 22], which further transmit them to motor neurons in the facial nucleus [Figures S2A–S2F, "FN"; termed MNs in 22] that project to vibrissa muscles via the facial nerve. The FNs are also innervated by three whisking central pattern generators (CPGs), which represent the tri-phasic CPG found in the BS, and which operate in an open-loop fashion [2, 22].

The BS-loop model consists of six types of elements [22]: (1) Neurons, which include TGs, TNs, and FNs. Both the TGs and TNs include four types of cells, according to the type of sensory input they relay: whisking (TG-W, TN-W), contact (TG-C, TN-C), pressure (TG-P, TN-P) and detach (TG-D, TN-D), where the contact-, pressure- and detach cells are collectively termed "touch cells" (TG-T and TN-T). Each subgroup of TGs innervates the corresponding subgroup of TNs. The FNs include three subgroups, according to the type of muscle they innervate: extrinsic protractor- (ExtP_MN), intrinsic- (Int_MN), and extrinsic retractor- (ExtR_MN) cells; (2) Mystacial pad muscles, which include three subgroups as the FNs: extrinsic protracting- (ExtP_muscle), intrinsic- (Int_muscle), and extrinsic retracting- (ExtR_muscle) muscles. Each muscle is innervated by the corresponding type of FNs; (3) Whiskers, which move in response to muscles contraction; (4) CPGs of three types, according to the type of FNs that they innervate: an extrinsic

protracting- (ExtP_CPG), intrinsic- (Int_CPG), and extrinsic retracting- (ExtR_CPG) CPG. The three types of CPGs periodically activate the three types of FNs in the following sequence: ExtP, Int, ExtR, resulting in smooth periodic protractions (triggered by ExtP+Int) and retractions (triggered by ExtR) [22]. Each CPG innervates the group of all FNs of the corresponding type that innervate all the whiskers on one side of the snout, to allow a coordinated motion of all ipsilateral whiskers (see Model assumptions); (5) Objects, which, if present in the whiskers' sweeping range, induce whisker-object contacts; (6) A manager, which acts as an external environment object that passes information between model's elements and supports technical issues. This component does not simulate any biological component directly.

H-Loop and Attentiveness Module

The H-loop represents the lemniscal pathways (see Model assumptions and Simulated TIP delays). The lemniscal pathways are disynaptic pathways [32–34] in which vibrissae-derived signals are transmitted from the TN to the thalamus, which further transmits them to the cortex. Thus, the H-loop is composed of two processing stations: a thalamic station (H1) and a cortical station (H2), and closes a loop with the BS-loop's TN station (Figures S2A–S2C).

The attentiveness module is assumed to be a putative brain area (Figures S2A–S2C, X) that closes a loop with the output station of the H-loop (H2) (see Model assumptions).

H1 and H2 are each divided into two subgroups, according to their functionality: attention-affecting cells (H1-att and H2-att), which can affect the attentiveness state of the attentiveness module (see Model assumptions), and TIP-affecting cells (H1-TIP and H2-TIP), which affect the activity of the TIP-generating TN-Ps (see Model assumptions; Figures S2A–S2C, pink and white regions in H1 and H2, respectively).

The H-loop is composed of the Neuron elements that already exist in the BS-loop model, while a new type of element was added for the modeling of the attentiveness module. The additional elements of the seventh-elements multiple-loop model are: (1) Neurons, of the input station (H1) and of the output station (H2) of the H-loop. The H1 cells, both H1-att and H1-TIP, are innervated by TN cells and project to the corresponding subgroups of H2 cells. The H2-att cells innervate the attentiveness module, while the H2-TIP cells innervate the TIP-generating TN-Ps (Figures S2A, S2B, and S2C, blue- and white TN-P, respectively); (2) Attentiveness modules (Xs), which close a loop with H2, by receiving inputs from H2-att cells and by projecting onto H2-TIP cells. The model includes two Xs, one for each side of the snout, such that each module is connected to all ipsilateral H2 stations that innervate the five rows of whiskers found on the same side of the snout (see Number of elements in the model).

Model Configurations

Three hypothesized TIP-regulation mechanisms were inspected, differing in the type of signals that could activate the H-loop (Figures S2A–S2C): (1) touch (pressure)-based enabling of BS-loop control ("pGATE+"): excitation of TIP-generating TN-Ps by the H-loop, whose activity could be triggered by whisker-derived touch (pressure) signals (Figure S2A, gray "P"), (2) whisking-based enabling of BS-loop control ("wGATE+"): excitation of TIP-generating TN-Ps by the H-loop, whose activity could be triggered by whisker-derived whisking signals (Figure S2B, gray "W"), and (3) restoration of BS-loop control ("GATE-"): inhibition of TIP-generating TN-Ps by the H-loop, whose activity could be triggered internally by X, independent of whisker-derived signals (Figure S2C).

In all three configurations, the cumulative stimulus that a given TIP-generating TN-P cell receives has to cross a threshold in order for the cell to successfully fire. In model configuration (1) and (2), the TIP-generating TN-Ps (Figures S2A and S2B, blue and white TN-P, respectively) are high-threshold cells, such that only a mutual stimulation by both of their pre-synaptic TG-P and H2-TIP cells (Figures S2A and S2B, TG-P and white H2, respectively) allows the TN-Ps to cross the threshold and fire (Figures S2D and S2E, respectively). In contrast, in model configuration (3), stimuli by the TG-Ps alone allow the low-threshold TIP-generating TN-Ps (Figure S2C, TN-P) to cross threshold and successfully fire, as long as their H2-TIP cells are silent and do not send inhibitory stimuli (Figure S2F).

In all three configurations, the activity of the H2-TIP cells depends on the activity of their attentiveness module (X), which in turn depends on its attentiveness state (see Model assumptions). In all three model configurations X becomes active when inattentive to object-exploration. In model configuration (1) and (2), when active, X constantly inhibits its H2-TIP cells, preventing them from firing in response to whisker-derived signals arriving via their H1-TIP cells, and hence from their high-threshold TN-Ps to generate TIPs. In contrast, in model configuration (3), when active, X continuously activates its H2-TIP cells, which constantly inhibit their low-threshold TN-Ps, preventing them from firing in response to their TG-Ps and to generate TIPs. In all three configurations, an inactive (i.e., attentive) X (Figures S2D–S2F, green rectangles) indirectly allows the post-synaptic TN-Ps (Figures S2D–S2F, blue or white TN-P) of its H2-TIP cells to generate TIPs in response to whisker-object contacts.

Simulated TIP Delays

GATE+

Both GATE+ mechanisms generated TIPs with extra delays relative to the BS-loop model. The extra delays resulted from the extra time it took the top-down inputs to travel along the H-loop until reaching the BS-loop TIP-generating TN-Ps relative to the relay time of the vibrissal-derived contact inputs along the BS loop. However, since in the pGATE+ mechanism both BS-loop- and H-loop-mediated inputs were triggered by touch (pressure) signals, the extra delays generated by this mechanism were larger than those generated by the wGATE+. In the latter, H-loop activation was triggered by whisker protraction, which in most contact conditions started early enough before whisker-object contact, to allow the minimal TIP delay possible, as generated by the BS-loop model (Table S4).

GATE-

In the GATE- mechanism blockage of inhibitory signals from the H-loop onto the BS loop was required for TIP generation. In this mechanism, the H-loop did not receive vibrissal inputs and its activity could be triggered by X alone. When touch-inattentive ($\overline{att}$), X continuously activated the H-loop cells (Figure S2C, dashed green line), which constantly inhibited the TIP-generating BS-loop cells (Figure S2C, dashed red line). When attentive, X, and thus also the H-loop regulated by X, were silent, allowing the TIP-generating BS-loop cells (Figure S2C, TN-P) to successfully fire in response to vibrissal-derived touch inputs without further delay.

Model Assumptions

BS-Loop Assumptions

(1) Each whisker is innervated by a separate sensorimotor feedback loop (BS-loop), to allow each whisker to affect its own motion [17]; (2) Although each whisker has some capability for independent movement, for simplicity, the whiskers on each side of the snout are assumed to move together [12, 15]; (3) TIPs are induced by the "E-R" configuration [22, model predictions]. Accordingly, ExtP- and ExtR FNs are innervated by TN-Ps and TN-Ds, respectively (in our BS-loop model both TN-Cs and TN-Ps innervate the ExtR_MNs [22]; see next point). Touch signals derived from pressure cells excite the ExtR_MNs and activate the corresponding muscles, resulting in a small and brief whisker retraction (TIP retraction); TIP retraction activates the detach cells, resulting in whiskers re-protraction [22, model predictions]; (4) Touch signals derived from pressure cells are necessary for TIP generation: TIP-onset time (relative to contact-onset time) depends on the radial distance of contact along the whisker [22, model predictions], which results from a similar dependency between the delays in the firings of TG-Ps and the radial distance of contact [35], suggesting that the pressure cells activity is required for TIP generation (whereas the delay in the firings of TG-Cs is fixed and is independent of the radial distance of contact [36]). For simplicity, pressure cell's activity is also assumed to be sufficient for TIP generation, without the necessity of contact-cells-derived signals (see Attentiveness module assumptions); (5) TN-Cs have a low activation threshold, allowing them to fire upon stimulations from their pre-synaptic TG-C cells and to affect their attentiveness module's attentiveness state (see Attentiveness module assumptions).

H-Loop Assumptions

(1) The higher loop (H-loop) regulates TIP generation by acting on the TIP-generating BS-loop's TN-Ps [37]. Although an alternative of the H-loop regulating TIP generation by acting directly on the FN is anatomically possible (see (3) below), we don't consider this possibility, since regulation of FN cells (FNs) is not specific to TIP regulation: since FNs activity is also required for the generation of the free-air whisking motion (see Sherman et al., 2013), regulating their activity would, undesirably, also affect free-air whisking (and see "Generality of the multiple-loop model"); (2) The H-loop is one of the lemniscal pathways: Rodent anatomy suggests three major candidates to implement the ascending pathway of the H-loop: trigemino-thalamo-cortical- (TTC), thalamo-striatal- (TS) and trigemino-olivo-cerebellar- (TOC) pathways [38]. We chose to model the H-loop as the TTC because (i) only the TTC is known to directly innervate the TIP-generating neurons in the BS-loop (Figures S2A–S2C, TN), whereas the others project to the output station of the BS loop (Figures S2A–S2C, FN) [17, 30, 32, 38–40] and are thus not specific for *TIP* regulation, and (ii) the TTC pathway closes the shortest (tri-synaptic) feedback loop with the BS loop, thus allowing the fastest response (i.e., TIP generation) to whisker-object contacts [39, and see Generality of the multiple-loop model]; (3) The activity of the H-loop can be triggered by either whisker-derived sensory signals or by the attentiveness module in the GATE+ and GATE- TIP-regulation mechanisms, respectively (see Model configurations). The whisker-derived sensory signals that can activate the H-loop in the GATE+ models are assumed to be either "whisking" or "touch": (i) the TGs that directly innervate the whiskers relay either whisking- (TG-W cells) or touch- (contact-, pressure- and detach TG-T cells) signals [36]; (ii) these two types of signals are relayed separately from the TG to the TN, and from the TN to the H-loop [41]; (iii) assume that either touch or whisking, but not both, can activate the H-loop, in order to compare two fundamentally different mechanisms, and in accordance with Yu et al. [41]; (iv) assume that out of the three "touch" signals, the "pressure" signals can activate the H-loop, in order to allow a simultaneous excitation of the TIP-generating high-threshold TN-Ps by both of their pre-synaptic sources: TG-P and H2-TIP; (4) for the GATE+ mechanisms, the choice of the specific lemniscal pathway is determined by the type of whisker-derived sensory signals that activate the H-loop (see Model configurations and previous point): either the lemniscal- or paralemniscal pathways in the pGATE+ or wGATE+ mechanisms, respectively; in the GATE- mechanism, the H-loop is also assumed to be one of the lemniscal pathways (paralemniscal), for a better comparison with the other mechanisms. Note that the H-loop is not necessary in this configuration, and was kept for consistency with the alternative mechanisms (and see Generality of the multiple-loop model); (5) Each BS-loop's TN station is innervated by a separate H-loop [17].

Attentiveness Module Assumptions

(1) The attentiveness module is assumed to be a putative center in the brain devoted to attention processing (but see Generality of the multiple-loop model); (2) Rat's attentiveness toward the object-exploration task is an internal, cognitive state of the rat, which can be affected by whisker-derived touch signals: when inattentive to the task, incoming touch (contact) signals originating from TG-Cs, and transmitted via the H-loop can switch the attentiveness mode to attentive. The externally-triggered switching is assumed to be a slow process, affecting H-loop's activity and hence also BS-loop's activity only in the whisking cycle that follows the cycle of whisker-object contact; (3) Rat's attentiveness is switched internally from attentive to inattentive after several cycles of whisker-object contacts, during which the rat is assumed to converge onto the object's feature that it aims to perceive [TIP-cluster statistics; 25, 38].

Generality of the Multiple-Loop Model

Model Architecture

As mentioned, to model TIP regulation we added to our earlier BS-loop model a higher regulatory loop (H-loop; Figures S2A–S2C, "H1" and "H2") and an attentiveness module (Figures S2A–S2C, "X"). While the former is implicated in other studies [e.g., 37], the latter can be modeled as an intrinsic state in each H2 neuron, instead of a separate neuronal module, without losing any of the behavior described here.

The Anatomy of the H-Loop

Among the several anatomical pathways that could constitute the ascending pathway of the H-loop (Model assumptions), we modeled the latter as the TTC pathways, which seemed to best fit the GATE+ regulation mechanisms. For better comparison of the GATE+ and GATE- models, the TTC pathways were also assumed for GATE-. However, the principles underlying GATE- largely accord with the 'action selection' mechanism of the basal ganglia (TS pathway) [42, 43]. Execution of the GATE- mechanism via the TS pathway should result in similar outputs, since the relay time of the H-loop in the GATE- model does not affect the response time of the TIP-generating TN-Ps (Figure S2F).

Since the H-loop's relay time does affect the response time of TIP-generating TN-Ps in the GATE+ mechanisms, these were also tested when executed via an optimal loop, which relayed the vibrissal-derived signals the fastest (1 ms from TN to H; 1 ms from H to TN). The optimal loop still resulted in persistent delayed TIP-generation by pGATE+ (Figures S1B and S1C, dotted blue), while abolishing the delays observed in the TTC-loop wGATE+ model: TIP-onset times in the optimal-loop wGATE+ model were similar to GATE- for all contact conditions (Figures S1B and S1C, dotted green), which is consistent with the TTC-based model, supporting its validity.

Favoring non-pGATE+ mechanisms is also the case in modeling: To allow the fastest response of the high-threshold TIP-generating TN-Ps in the pGATE+ configurations, TG-Ps had to innervate matching pairs of low- and high-threshold TN-Ps. In the wGATE+ and GATE- configurations no such constraints were needed. The less-constrained connectivity makes the latter more probable to occur during development.

Top-Down Projections from H-Loop to BS-Loop

As mentioned, we assume that the H-loop regulates TIP generation by acting on the TNs. Although it has been shown that wM1 directly projects on the FN we do not consider the possibility of the H-loop directly regulating the FN due to several reasons, as indicated in "H-loop assumptions". Briefly, since FN cells are involved in on-going whisking control, their attention-driven modulation should be specific to specific inputs from the TN – such a requirement has no experimental support and is thus not justified at this stage of the modeling.

TIP Delays

The extra TIP delays generated in the GATE+ models follow from the relay time along the H-loop, whose output was required for TIP generation. This time resulted from three model parameters. While the values of all these appear in the literature for the wGATE+ model, only two are available for pGATE+ (Table S4). To obtain the shortest extra delay possible in pGATE+, the third was assigned the minimal value possible (1 ms). Assuming another, necessarily larger, value (e.g., 12-14 ms as in wGATE+) would have increased the extra delay (e.g., ~19 ms). Hence, the extra delay reported for pGATE+ is a lower bound. In contrast, the average extra delay reported for wGATE+ during small contact angles is based on biological data and hence constitutes a solid estimation. Finally, we stress that the GATE- model did not generate such extra TIP delays, regardless of the choice of parameter values, since here H-loop output was not required for TIP generation.

Triggering X by Whisker-Derived Inputs

In all TIP-regulation mechanisms we tested (Model configurations), the attentiveness module was triggered by inputs from contact cells. Although using inputs from pressure cells would not affect our results, the fast arrival of inputs from the contact cells is consistent with the fast and brief responses of layer 4 neurons in S1 to whisker-object contacts [44].

Number of Elements in the Model

The multiple-loop model contains two sets of five rows of whiskers, representing the two whisker pads located at each side of the snout in the rat [45, 46]. The five rows include two rows of four whiskers and three rows of seven whiskers, corresponding to rows A-B and C-E in the rat [1A, 22]. In both types of rows, each whisker is attached to several muscles [1B, 22].

In addition, each whisker is innervated by a separate pool of neurons that closes a loop between that whisker and the muscles attached to it (BS-loop; STAR Methods, Model assumptions [3A, 22];), and by a separate pool of neurons that closes a loop with the whisker's TN cells (H-loop; STAR Methods, Model assumptions).

Finally, the multiple-loop model also contains two sets of three CPGs (ExtP, Int, ExtR, see Model elements) and two attentiveness modules (Xs). Each set of CPGs and each X innervates all the FNs and all H2-TIPs that innervate the five rows of ipsilateral whiskers, respectively, resulting in a separate control over whisker motion in each whisker pad.

The Modeling Tools: Statecharts, Rhapsody, MATLAB

As mentioned, the models contain several types of elements. The behavior of each of these is described by a statechart, as discussed in [22]. In addition to its own statechart, each type of element possesses a separate set of parameters. During model execution, many copies of each type of statechart are generated, one for each element, together with a separate set of parameters initialized uniquely for each element. Model execution is performed by using the Rhapsody tool [29], which executes the behaviors defined by the various

statecharts collectively, giving rise to a dynamic simulation of the entire systems, allowing interactions between the various elements and their behaviors, and which can change the states and parameter values of elements at run time. The values of the model parameters, together with their sources, are specified at https://www.weizmann.ac.il/neurobiology/labs/ahissar/sites/neurobiology.labs.ahissar/files/uploads/sherman_tip_2017_si_model_parameters.pdf. The statecharts of the BS-loop model's elements are described in [22]. The statechart of the newly-added attentiveness module (X) is described below.

The Statechart of the Attentiveness Module

For the exemplary output presented in Figure S1A, one copy of the statechart was generated at the beginning of the simulation, and the rat was initially inattentive to the object (see Figure S2G). The first contact triggered a delayed switching to an attentive state, such that TIPs were generated from the second contact cycle on. After three contact cycles the rat converged onto the assessed feature of the object and internally switched back to the inattentive state. The rat "ignored" future contacts and did not respond (i.e., did not move to the attentive state despite contact events), resulting in no TIPs for a pre-defined period of time (*minPerceivingTime*), which was set to zero in the simulation. Thus the first contact that followed the first TIP cluster (cycle 5) triggered a delayed switching into the attentive state, re-generating TIPs from the following contact cycle (cycle 6), and so on.

QUANTIFICATION AND STATISTICAL ANALYSIS

The statistical analyses performed in this study, together with the analyzed variables, are specified in METHOD DETAILS. Only encountering episodes in which all classifications of two independent observers were fully matched were included in the analyses. None of the analyses included all of the episodes (n = 115 and 40 first- and late episodes, respectively). The inclusion criteria and the sample size for each analysis are specified in METHOD DETAILS, Results and Discussion, and figure legends. Dispersion of the analyzed variables and statistical test scores are specified in the figures and in Results and Discussion. *Z*-test was always used unless mentioned otherwise. The data met the required assumptions for performing each of the statistical tests performed in this study.